Processing Notes: MOSAiC Helicopter-borne Electromagnetic Ice Thickness Measurements

Luisa von Albedyll, Christian Haas, Raphael Grodofzig

The MOSAiC HEM data set comprises of 23 flights conducted between September 30, 2019 and September 28, 2020. There were three main patterns: floe grids over the central observatory (CO), Butterfly patterns covering the distributed network (DN) and large-scale transects or triangles. An overview of dates and patterns are listed in Tab.1

Tab. 1: Flight parameter

Date	ID	Pattern
20190930_01	AF122/1_3-3	DN
20191013_01	AF122/1_3-4	DN
20191014_01	AF122/1_3-5	CO and DN
20200404_01	PS122/3_34-93	North triangle
20200404_02	PS122/3_34-94	South triangle
20200410_01	PS122/3_35-91	CO floe grid
20200417_01	PS122/3_36-156	Butterfly
20200426_01	PS122/3_37-137	Butterfly
20200619_01	PS122/4_44-95	EM-Bird large scale gradient
20200621_01	PS122/4_44-127	Butterfly (2 triangles)
20200621_02	PS122/4_44-128	Butterfly (1 triangle) + N-S Transect
20200622_01	PS122/4_44-130	Butterfly (1 triangle) + S-N Transect
20200630_03	PS122/4_45-38	N-S Transect
20200701_01	PS122/4_45-54	Butterfly (2 triangles)
20200707_04	PS122/4_46-40	EM-Bird floe map
20200806_02	PS122/4_50-37	S-N Transect
20200807_02	PS122/4_50-47	Transect
20200818_01	PS122/5_59-180	Triangle pattern
20200907_02	PS122/5_61-56	square around CO
20200908_01	PS122/5_61-61	square around CO
20200917_01	PS122/5_62-151	two triangles from ship
20200928_01	PS122/5_63-117	transect S-N

The flights were processed using the software IGOR64 (version 8.04) and the corresponding ISIT packages (Hendricks and Haas, unpublished, following Haas et al. 2009). To remove the instrument drift, most of the times an automatic procedure was used that fits a polynomial to all measurement points from an altitude higher than 85 m. For a few occasions, this fit was applied not to the whole data set in a file, but section-per-section. In exceptions, the polynomial was fitted manually by choosing offset, curvature, and slope.

In a second processing step, gain and phase were adapted. Guidance was provided by:

- Continuity: If possible, gain was kept as similar to the previous sections as was reasonable

- Open water areas (as indicated by events and in the protocols): should have zero thickness
- Positive thickness: no negative thicknesses should occur
- Good agreement of inphase and quadrature thickness
- Shape of ITD: no secondary “shoulders” or modes

Depending on how well the above-mentioned criteria could be met, a quality flag was assigned to each data file, called “reliability” indicating the classification:

1: excellent
1.5: very good
2: with uncertainty
2.5: with large uncertainty
3: not possible to process

For a few occasions, the strong instrument drift leading to unstable EM signals and hampered proper drift corrections, making measurements at low flying altitude unreliable. This data that was assigned a 2 or larger and it was identified by large undulations in the high-altitude flight phase in which the signal is supposed to be stable.

The quality was further checked by comparing the processing results of two different persons. Data files with deviations in mode, standard deviation, mean, as well as large visual differences in the shape of the ITDs were discussed (see Tab.2). Large deviations combined with reliability flags below 1.5 where identified.

Tab. 2: Quality assessment of flights: Two ITDs obtained by two persons processing were compared in respect to mode, mean, and standard deviation.

Flights with good agreement in ITD	14.10, 4.04 (2), 10.4, 17.04, 19.06, 1.07, 7.07
Flights with minor deviations in ITD	4.4 (1), 26.04, 30.4, 21.06 (1), 21.06 (2), 22.06, 30.6
Flights with major discrepancies, discarded	30.09, 13.10, 6.08, 7.08

Post-processing and quality control

To study the potential impact of the medium quality data sets, we compared (1) the statistical differences between ice from the same flight but different location and different quality flags and we compared (2) ice from different flights but approximately the same locations.

(1) We did not find a systematic offset between medium and good sections. Mean thickness differed by on average 6.5 cm or 1-2% (Tab.3). The maximum deviation of 19 cm was found on 2020-07-07.

Tab. 3: Example of the comparison table for the flights on 2020-06-21.

	Medium	Good
Mean / m	2.342	2.386
Mode / m	2.0	2.0
FWHM / m	1.0	1.0
e-fold	0.761	0.838
Coverage / %	100.0	37.6
Crit. length / km	20.6	
Crit. length / %	5.8 #with respect to the entire day	

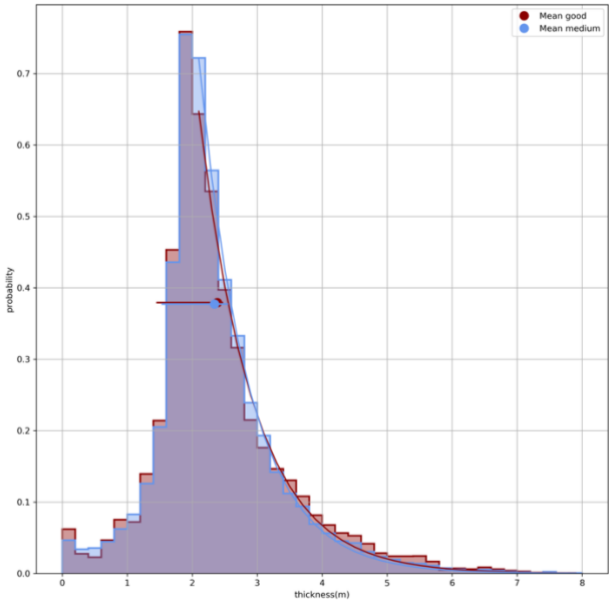

Figure 1: Ice thickness distribution of medium and good quality parts of the flights on 2020-06-21.

(2) On June 21 and June 21, 2020, the flight tracks overlapped three times sufficiently close to compare the ITDs (Fig. 2). All sections were long enough to be representative (see Rabenstein et a. 2010 for definition) except of section 2 on June, 22 (Fig. 2). The two flights from June 21 differed by max. 11 cm (Section 1, 2), while the flight from June 22 (Section 1, 2) deviated on average by 29 cm (Fig. 3). Despite the fact that the temporal difference and hence also the spatial variability might be larger between the flights of different dates, this raises concerns about the reliability of the June 22 flight. We suggest further quality control before using this flight.

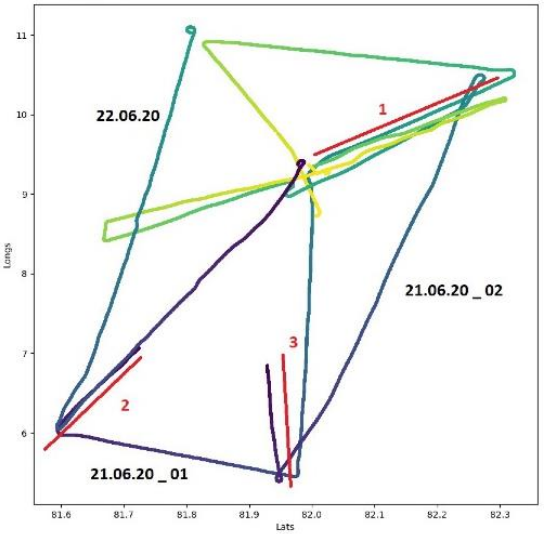

Figure 2: Flight tracks on June 21 (two flights) and June 22. Overlapping sections are marked in red and numbered 1-3

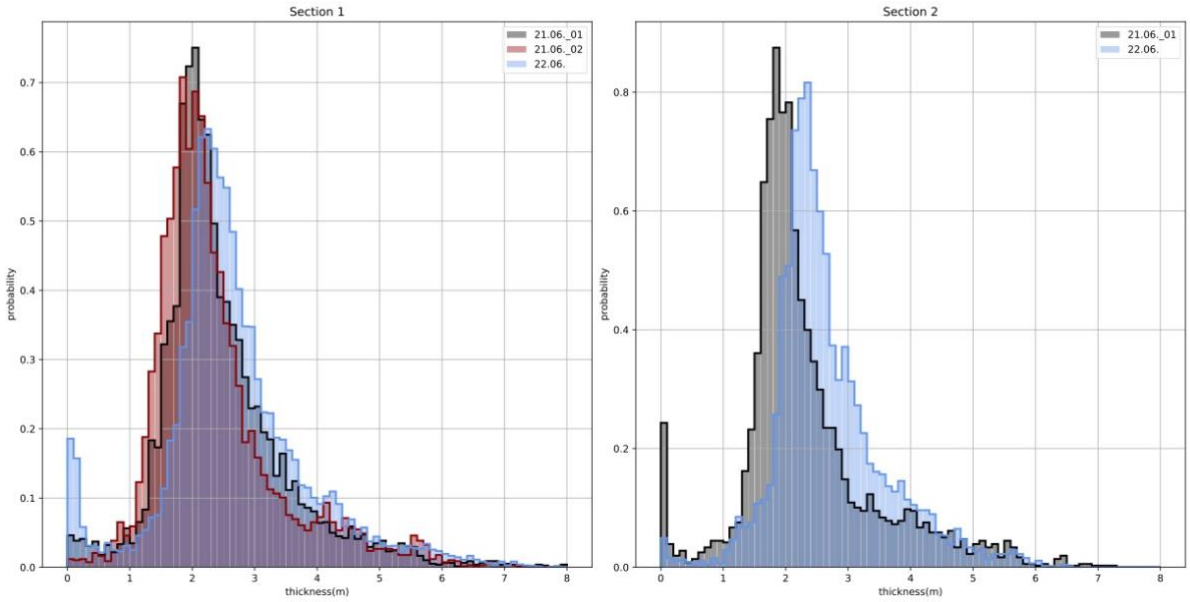

Figure 3: ITDs of overlapping sections from two flights on June 21 and June 22, 2020.

Spike Filter

Spikes at the beginning and end of high-altitude calibration flights are removed using a moderate and a strict filter. The spikes are characterized by an almost monotonic increase (before ascent) or decrease (after descent) in ice thickness spanning over several data points. Thickness is often as high as the maximum thickness of the section and is prone to bias the mean, maximum and standard deviation of the ice thickness (see Fig.2).

The filter cuts out all data points which follow at least 20 NaN values during descent (or which are followed by at least 20 NaN values during ascent), and additionally meet one of the following conditions:

1. For 7 out of 10 values, the ice thickness gradient is positive (negative) which points to an unphysical, monotonous increase (decrease)
2. The mean of 20 values is higher than 3 times the median of the total data set (moderate filter), or higher than 2 times the median of the total data set (strict filter).

The effects of the filters are visualized in Fig. Whether a data point is filtered out by the strict or moderate filter, is indicated in the all_final files. Remaining data points are denoted by 1, deleted ones by 0 for the respective filter.

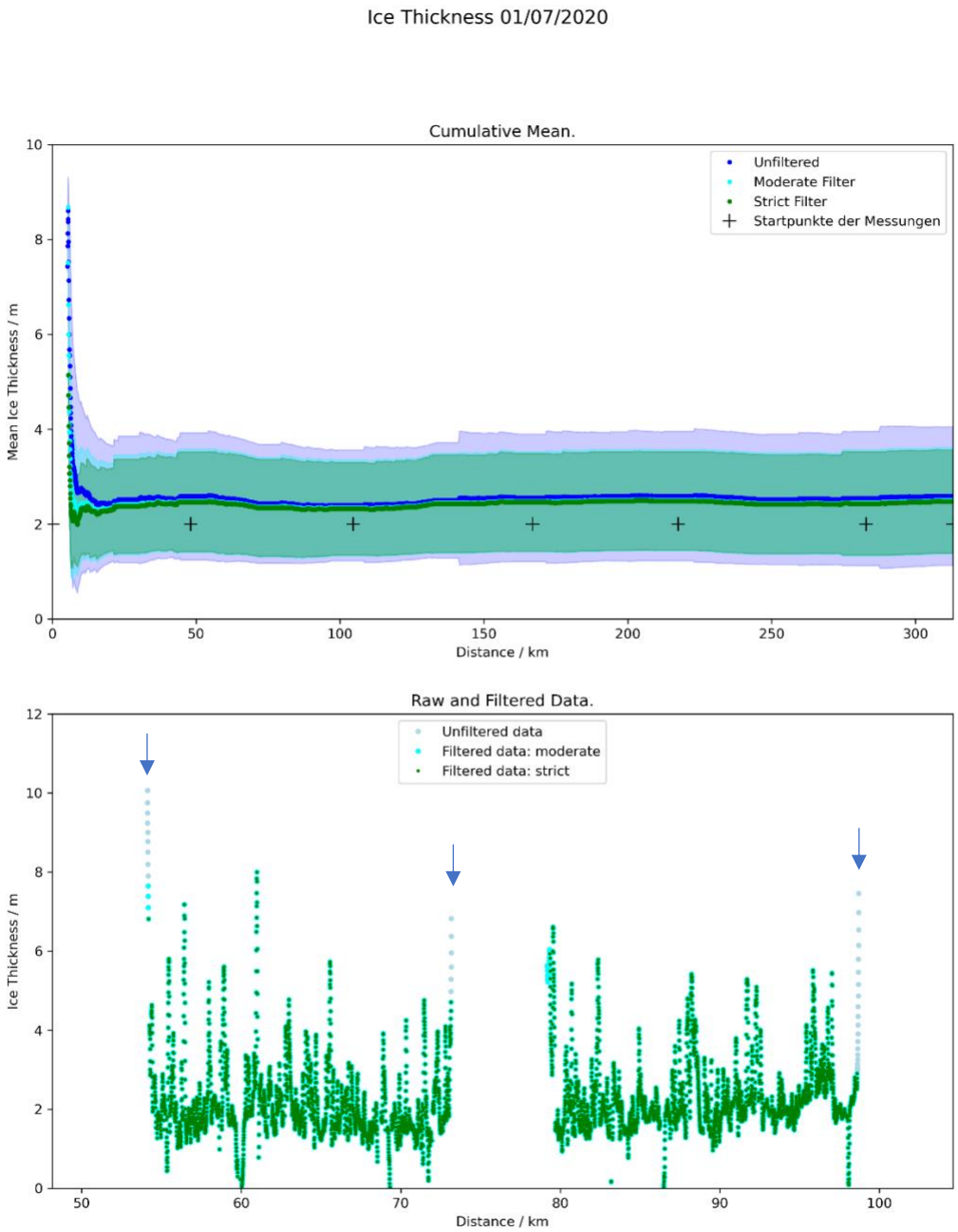

Figure 4: Illustration of unfiltered and filtered data (lower panel). The effect of the filters can be seen best in a the cumulatively averaged ice thickness plot (upper panel). Mean and standard deviation contain unnatural "steplike" jumps for the unfiltered data. The filters contribute to the "smoothness" of the cumulatively averaged ice thickness by removing the unnatural spikes.

Visual control via GoPro Images

GoPro footage taken during the flight on July 1st was used to check visually the uncertainty of the thickness data. Particularly in leads, visible on the Go-pro images, the ice thickness is expected to be zero or at least below the measurement uncertainty of the EM Bird (± 10 cm). For this purpose, the images were projected, georeferenced and plotted along the flight track. Unfortunately, the lack of precise height information hampered a precise

analysis. Nevertheless, we were able to estimate the image extensions and accomplish a rough visual quality check.

In general, we found a good agreement in leads between the GoPros and the EM-thicknesses (Fig. 5, 6). When there was a disagreement, the leads were small (< 50 m) or the imprecise geolocation did not exclude that the locations of EM measurements were over sea ice close by. The ice thickness is overestimated at roughly 20 % of the leads. We could not find a trend of disagreement in location or flight distance.

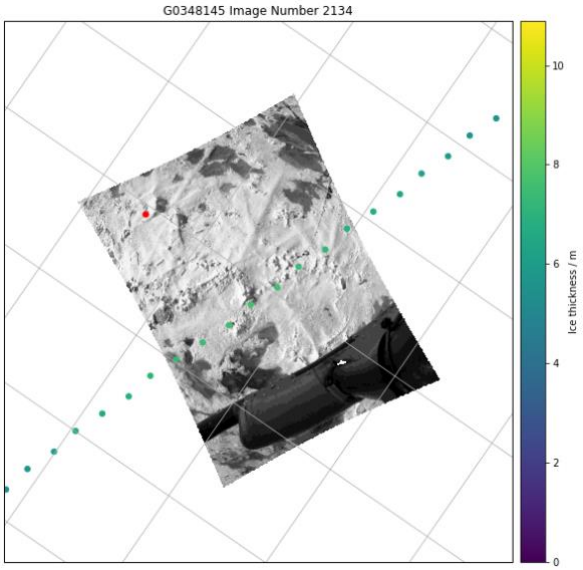

Figure 5: Georeferenced GoPro Image of a ridge.

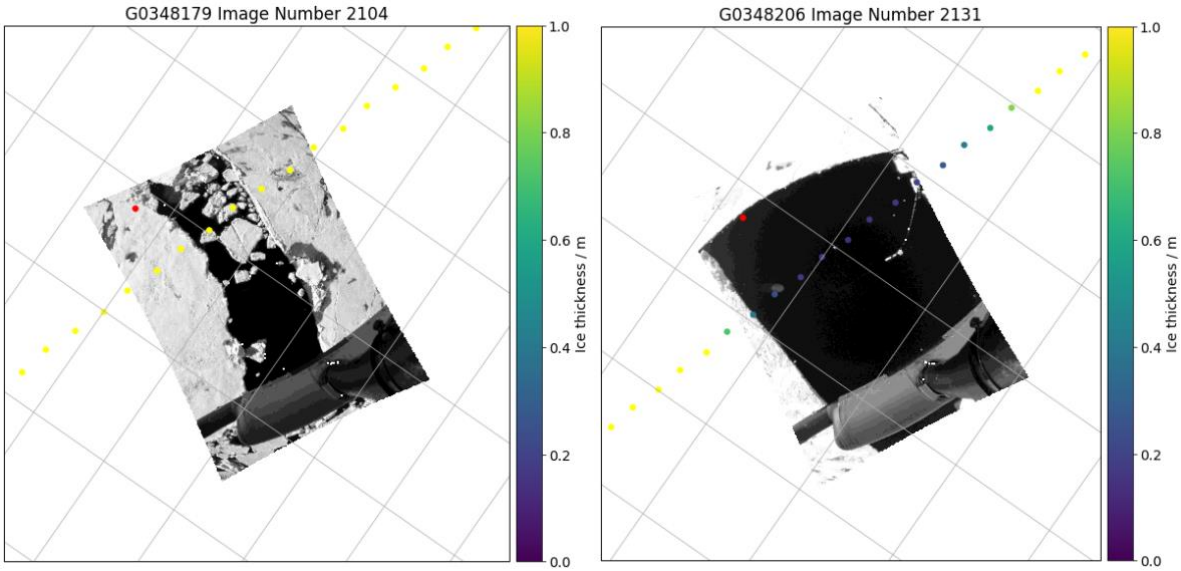

Figure 6: Undetected (left) and detected(right) leads. The extent of the undetected lead in flight direction is <50 m.

References:

Haas, C., Lobach, J., Hendricks, S., Rabenstein, L., and Pfaffling, A.: Helicopter-borne measurements of sea ice thickness, using a small and lightweight, digital EM system, J. Appl. Geophys., 67, 234–241, https://doi.org/10.1016/j.jappgeo.2008.05.005, 2009.

Rabenstein, L., Hendricks, S., Martin, T., Pfaffhuber, A., and Haas, C.: Thickness and surface-properties of different sea-ice regimes within the Arctic Trans Polar Drift: Data from summers 2001, 2004 and 2007, J. Geophys. Res., 115, C12059, https://doi.org/10.1029/2009jc005846, 2010.